Separation Science and Technology
Publication details, including instructions for authors and subscription information:
http://www.informaworld.com/smpp/title~content=t713708471

Orientation of Rigid Macromolecules during Hydrodynamic Chromatography Separations

Robert K. Prud'homme[a]; David A. Hoagland[a]
[a] DEPARTMENT OF CHEMICAL ENGINEERING, PRINCETON UNIVERSITY, PRINCETON, NEW JERSEY

To cite this Article Prud'homme, Robert K. and Hoagland, David A.(1983) 'Orientation of Rigid Macromolecules during Hydrodynamic Chromatography Separations', Separation Science and Technology, 18: 2, 121 — 134

To link to this Article: DOI: 10.1080/01496398308055664

URL: http://dx.doi.org/10.1080/01496398308055664

SEPARATION SCIENCE AND TECHNOLOGY, 18(2), pp. 121–134, 1983

Orientation of Rigid Macromolecules during Hydrodynamic Chromatography Separations

---

ROBERT K. PRUD'HOMME and DAVID A. HOAGLAND

DEPARTMENT OF CHEMICAL ENGINEERING
PRINCETON UNIVERSITY
PRINCETON, NEW JERSEY 08544

Abstract

We have recently reported the successful separation of xanthan polysaccharide macromolecules by hydrodynamic chromatography. We show here that kinetic theory calculations of the orientation of rodlike macromolecules by flow in porous media can be used to intepret the experimentally observed chromatographic separations. Xanthan is a rigid rodlike molecule approximately 1 μm in length and 40 Å in diameter, yet it is found experimentally to elute from the chromatography column at the same volume as a 0.153-μm diameter latex sphere. To relate the physical dimensions of the xanthan molecule to its "apparent hydrodynamic volume" as determined from chromatography experiments, we begin by modeling the molecule as a rigid dumbbell. Elongational strain rates and shear rates characteristic of flow through a packed bed of impermeable 25 μm spheres are calculated and subsequently used to obtain the orientational distribution function for the dumbbell in elongation and shear. The projection of the distribution function in the direction of flow is evaluated to determine an effective radius (or cross section) for the oriented dumbbell. In elongation the effective diameter is 0.14 μm; in shear the effective radius is 0.22 μm. These values compare favorably with the experimentally determined value of 0.153 μm. The analysis predicts the effects of flow rate and packing diameter on the separations of nonspherical particles by hydrodynamic chromatography. In addition, the analysis provides a framework for investigating the maximum size rigid macromolecule that can pass through a porous media of given characteristics. The success of these order-of-magnitude calculations suggests that a more detailed analysis of the orientation in the complex two-dimensional flow field in a pore will prove fruitful.

INTRODUCTION

There is considerable interest in chromatographic separation of ultrahigh molecular weight water soluble polymers. Also, there is interest in the flow of

0149-6395/83/1802-0121$3.50/0

polymers through porous media in enhanced oil recovery. The physics involved in both processes—the flow of a polymer molecule through a chomatographic packing and the flow of a polymer molecule through a porous rock structure—are similar. We have recently shown that hydrodynamic chromatography can be used to determine the molecular sizes of rigid ultrahigh molecular weight xanthan polysaccharides. We have described the molecular structure of xanthan and the details of the hydrodynamic chromatographic packing and the flow of a polymer molecule through a given here. The purpose of this paper is to show that polymer kinetic theory calculations can be used to relate the location of the chromatograhic peaks to the molecular dimensions of rodlike xanthan molecules. The shear and elongational flows in the hydrodynamic chromatography column cause significant orientation of the xanthan molecules which can be predicted from kinetic theory calculations. The predictions, based on upper bounds for the shear and elongational fields in the column, are in good agreement with experimental results.

BACKGROUND ON XANTHAN POLYSACCHARIDES AND HYDRODYNAMIC CHROMATOGRAPHY

Xanthan is a high molecular weight extracellular polysaccharide produced by *Xanthomonas campestris* bacterium during fermentation. It is widely used as a viscosifier in paints and foods, and is under study as a mobility control agent in enhanced oil recovery. The interesting rheological properties of xanthan are a result of its rigid rodlike conformation (*2–4*) and high molecular weight [2–50 million, apparently depending on fermentation conditions and the degree of self-aggregation (*2, 5*)]. The extended conformation makes xanthan too large for conventional size exclusion chromatography (SEC or GPC). Our work has shown that this nonspherical, ultrahigh molecular weight macromolecule can be separated by hydrodynamic chromatography.

Hydrodynamic chromatography is a particle size measuring technique that has been used to study spherical latex particles in the range $0.05\ \mu m < D < 1.0\ \mu m$ (*6–8*). The apparatus, shown in Fig. 1, is similar to that used in size exclusion chromatography except for the column packing. In hydrodynamic chromatography rather long columns (1–3 m) are packed with impermeable spheres having a narrow size distribution (20 ± 3 to $40 \pm 5\ \mu m$ diameter). A latex sample is injected into the column and it is found that larger latex spheres elute from the column before smaller spheres. The separation is caused by larger particles preferentially sampling regions of faster moving fluid in the nonhomogeneous velocity field. The mechanism of

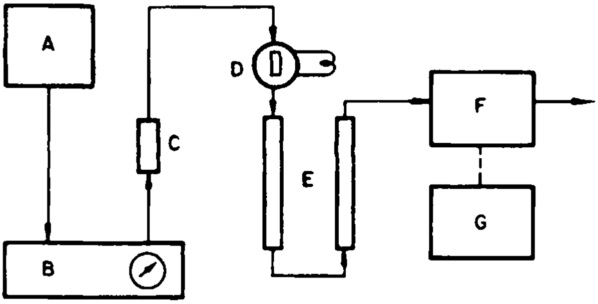

FIG. 1. Hydrodynamic chromatography apparatus. A: Solvent reservoir. B: High-pressure liquid chomatography pump. C: Column prefilter. D: Loop sample injection valve. E: Columns 4.6 mm i.d. × 1 m. F: Fluorescence detector. G: Strip-chart recorder.

separation for spherical particles has been discussed by Silebi and McHugh (*7*).

Our experiments, reported in detail elsewhere (*1*), involved calibrating a hydrodynamic chromatography column with monodisperse latex spheres by determining the elution volume as a function of sphere diameter. Fluorescently tagged, purified xanthan was injected into the column and was found to elute at the same volume as a 0.153-μm diameter sphere. An example of the separation is shown in Fig. 2, where native xanthan and a small molecular weight marker species were simultaneously injected. The degree of separation is given by the retention factor R_f which is defined by $R_f = V_m/V_p$, where V_m is the elution volume of the marker and V_p is the elution volume of the xanthan peak. When the xanthan is reduced in molecular weight by sonication, the xanthan and marker peaks move closer together, as would be expected.

The molar volume of a 0.153-μm sphere is 1.1×10^6 dL/gmol whereas the molar volume of xanthan as determined from intrinsic viscosity measurements is 1.4×10^8 dL/gmol, and the molar volume calculated from the contour length and diameter of the xanthan molecule is 7.8×10^3 dL/gmol (*9, 10*). This suggests that xanthan must be significantly oriented during flow for it to elute at the same volume as a 0.153-μm latex sphere. This is shown in Fig. 3.

We will now show how polymer kinetic theory calculations prove useful in explaining the observed hydrodynamic chromatography separations of xanthan. These calculations allow us to relate the retention factors of the latex calibration spheres to the dimensions of xanthan molecules oriented by the flow field.

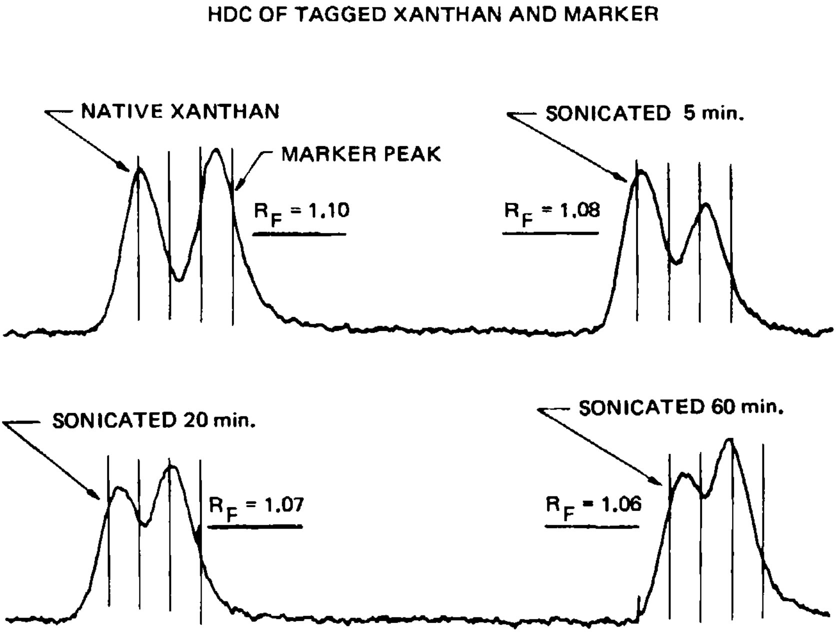

FIG. 2. Hydrodynamic chromatography separation of xanthan polysaccharide. The separation of native xanthan from a small molecular weight salt marker is shown. Upon sonication the xanthan is degraded and the xanthan peak moves closer to the marker peak.

KINETIC THEORY MODELING OF XANTHAN ORIENTATION IN FLOW

The solution properties of a rodlike macromolecule such as xanthan can be qualitatively predicted using a rigid dumbbell model for the polymer. From order of magnitude estimates for the flow parameters in a hydrodynamic chromatography column, the orientation of a xanthan molecule (represented by the dumbbell model) can be analyzed as the molecules moves through a constricted pore in the packed bed (Fig. 4). Of interest here is the effective "size" of the molecule—the degree to which the flow field aligns the molecule.

Two sets of coordinates, external and internal, will describe the position of the polymer and its orientation, respectively. In a packed bed of spheres the flow field as described by external variables is rather complex. However, the converging and diverging interstitial regions between the packing particles

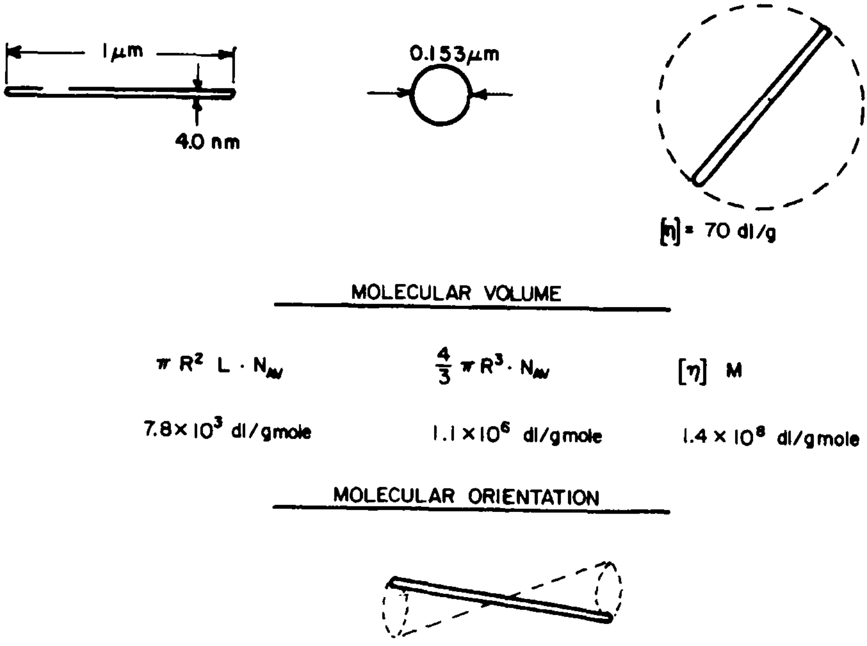

FIG. 3. Comparison of volume occupied by xanthan molecules and spheres. The xanthan elutes from the column at the same volume as a 0.153-μm sphere. This indicates significant orientation of the xanthan by flow.

can be modeled as a periodically constricted tube. Reasonable bounds for the orientation of the polymer molecule can then be obtained by calculating the orientation in the region dominated by shear—the tube wall—and in the region dominated by elongational flow—the tube centerline. In what follows we calculate values for the shear rate and elongational strain rate in the interstitial regions of the packed bed, and then perform kinetic theory calculations of the degree of orientation of molecules near the tube wall and molecules on the tube centerline. The internal coordinate system for the molecular model, and a particular representation of simple shear and elongational flows, are given in Fig. 5.

Excluding electrostatic and intermolecular potentials, only hydrodynamic and Brownian forces will act on the dumbbell. The hydrodynamic forces will tend to align the molecule in the flow while the Brownian forces will oppose the tendency for alignment. Since the Brownian effect is statistical in nature,

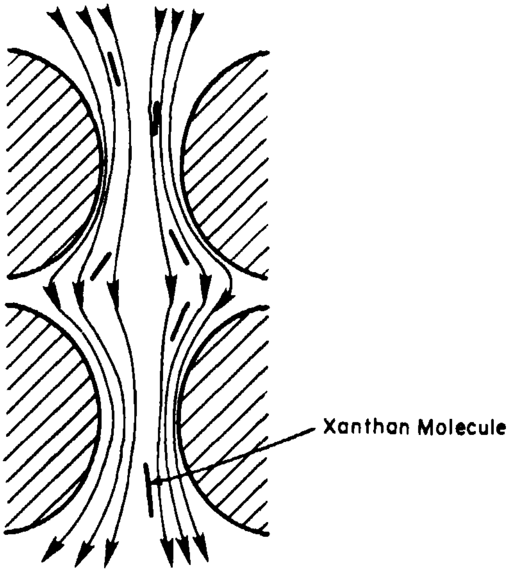

FIG. 4. Possible orientation of xanthan in flow through a porous medium.

a distribution function $\psi(\theta, \phi)$ will be required to describe the dumbbell's orientation. This function will obey the normal equation of continuity and a "diffusive" equation of motion (*11, 12*):

Continuity:

$$\frac{\partial \psi}{\partial t} = -\frac{1}{\sin\theta}\frac{\partial}{\partial\theta}(\dot{\theta}\sin\theta\,\psi) - \frac{\partial}{\partial\phi}(\dot{\phi}\,\psi) \tag{1}$$

Motion:

$$\begin{aligned}\frac{\partial \psi}{\partial t} = {} & \frac{1}{\sin\theta}\frac{\partial}{\partial\theta}\left[\frac{\sin\theta}{6\lambda}\frac{\partial}{\partial\theta}(\psi) - \sin\theta(\boldsymbol{\kappa}{:}\boldsymbol{\delta}_R\boldsymbol{\delta}_\theta)\psi\right] \\ & + \frac{1}{\sin^2\theta}\frac{\partial}{\partial\phi}\left[\frac{1}{6\lambda}\frac{\partial}{\partial\phi}(\psi) - \sin\theta(\boldsymbol{\kappa}{:}\boldsymbol{\delta}_R\boldsymbol{\delta}_\theta)\psi\right]\end{aligned} \tag{2}$$

where $\boldsymbol{\delta}_R$ and $\boldsymbol{\delta}_\theta$ are unit vectors, $\dot{\theta}$ and $\dot{\phi}$ are the rate-of-change of the θ and ϕ coordinates, $\boldsymbol{\kappa}$ is a tensor that describes the homogeneous velocity field

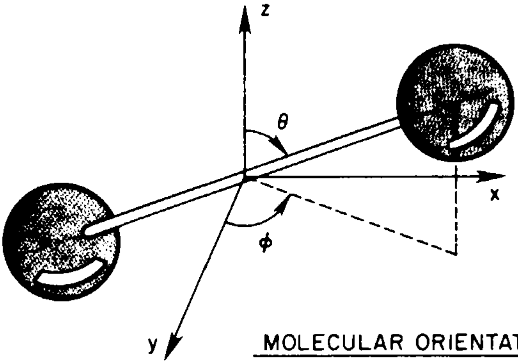

MOLECULAR ORIENTATION

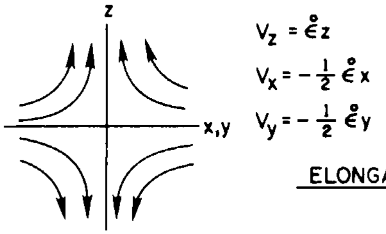

ELONGATIONAL FLOW

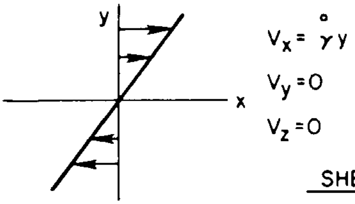

SHEAR FLOW

FIG. 5. Relationship between rod orientation and flow fields. Orientation is described by internal coordinates θ and ϕ, while flow fields are described in terms of external coordinates X, Y, and Z.

$\mathbf{v} = \boldsymbol{\kappa} \cdot \mathbf{r}$, and λ is a time constant characteristic of the dumbbell's rotational diffusion (it will be determined experimentally for a particular polymer). While a rigid dumbbell is the model used here, other slender axisymmetric particles will obey the same equation of motion with a suitably selected definition of λ. There will also be a normalization condition for $\psi(\theta, \phi)$:

$$1 = \int_0^{2\pi} \int_0^{\pi} \psi(\theta, \phi) \sin \theta \, d\theta \, d\phi \tag{3}$$

The function $\psi(\theta, \phi)$ must be finite and single-valued within the domain of interest ($0 \leq \theta \leq \pi$, $0 \leq \phi \leq 2\pi$). Steady-state solutions to this set of equations have been obtained for the two cases of interest, simple shear and elongation.

Elongation

The normalized orientational distribution function $\psi(\theta, \phi)$ can be calculated analytically for steady elongational flow* using the equation of motion (*11, 12*). In this case $\psi(\theta, \phi)$ reduces to $\psi(\theta)$ since the flow has symmetry about the z-axis.

$$\psi(\theta) = \frac{\exp(9\lambda\dot{\varepsilon}(\cos^2\theta)/2)}{2\pi\int_0^\pi \exp(9\lambda\dot{\varepsilon}(\cos^2\theta)/2)\sin\theta\, d\theta} \tag{4}$$

As the molecule flows through a constricted pore, the effective size of the dumbbell will be given by a projection of $\psi(\theta)$ onto a plane perpendicular to flow. The angular distribution function of this projection will be given by

$$\psi_p(\theta) = \psi(\theta)\sin\theta \tag{5}$$

The maximum value of $\psi_p(\theta)$ will qualitatively describe an effective projected diameter for the dumbbell,

$$D_{\text{eff}} = l\sqrt{1/9\lambda\dot{\varepsilon}} \tag{6}$$

where l is the length of the dumbbell. The average diameter $\langle D \rangle$ might also be defined,

$$\langle D \rangle = \frac{l\int_0^\pi \exp(9\lambda\dot{\varepsilon}(\cos^2\theta)/2)\sin^2\theta\, d\theta}{\int_0^\pi \exp(9\lambda\dot{\varepsilon}(\cos^2\theta)/2)\sin\theta\, d\theta} \tag{7}$$

---

*Actually the elongational strain is not steady along the centerline of the periodically constricted tube but oscillates between converging and diverging flow as the tube radius converges and diverges. However, the uniaxial converging flow is more effective at aligning molecules than is the biaxial flow in the diverging section. Therefore, using an estimate of the elongation rate in the region of converging flow for the kinetic theory calculation appears justified for this initial order of magnitude calculation. The agreement between these predictions and our experimental observations provides tentative support for the approximation. In addition we are currently performing the calculations for orientation of a rodlike particle in an oscillatory elongational field.

The rotational diffusion time constant consistent with the dumbbell model can be estimated for xanthan molecules from experimental data using an expression involving the intrinsic viscosity (*11*):

$$\lambda = \lim_{\dot{\gamma} \to 0} \frac{\eta_s M[\eta]_0}{\bar{N}kT} \tag{8}$$

where M is the molecular weight $\sim \times$ 10 g/gmol
$[\eta]_0$ is the intrinsic viscosity $\sim$70 dL/g
$\tilde{N}$ is Avogadro's number
k is Boltzmann's constant
T is the temperature $\sim$298 K
η_s is the solvent viscosity $\sim$0.01 g/cm·s

The molecular weight and intrinsic viscosity data listed above were obtained by Wellington (*9*) and appear to be the best literature values. With these values, λ is 0.0056 s.

The strain rate will be calculated from the complicated velocity profile in the interstitial area of the bed. Payatakes and Neira (*13*) have modeled pores in such a bed of packed spheres as periodically constricted tubes; with this model, the creeping flow problem for Newtonian fluids was solved using collocation (*14*). Employing the solution of Payatakes et al., an order of magnitude estimate of $\dot{\varepsilon}$ can be made for a hydrodynamic chromatography column with typical operating parameters. The equivalent constricted pore is shown in Fig. 6 alongside the values used in the calculation. The values of r_1^* and r_2^* are taken from Payatakes and Neira (*13*) and are experimental values for a randomly packed bed of glass spheres (particle diameter 470 μm, porosity 0.38). The strain rate is estimated from the difference in velocities, $V_2 - V_1$, divided by the distance between the points 1 and 2, $D_p/2$. The resulting value of $\dot{\varepsilon}$, 1200^{-1}, when substituted in Eq. (6), yields $D_{\text{eff}} = 0.14$ μm for a xanthan molecule of length 1.0 μm [Wellington estimated the length of xanthan molecules in dilute salt solutions as 0.7 to 1.0 μm (*9*)]. The corresponding value of the average diameter, $\langle D$, as defined by Eq. (7), is 0.08 μm. In Figs. 7 and 8, $\psi(\theta)$ and $\psi_p(\theta)$, respectively, are plotted for this set of parameters.

Shear Flow

The solution to the diffusive equation of motion for shear flow is considerably more difficult since the flow is no longer axisymmetric. Stewart

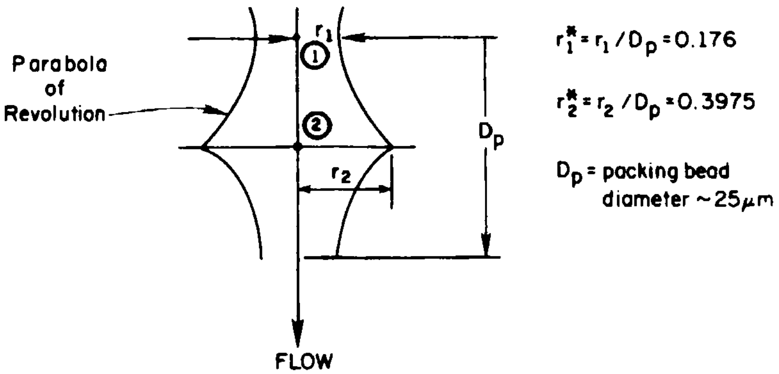

FIG. 6. Pore structure in a bed of spheres. The pore model of Payatakes and Neira is shown alongside their experimental values for the geometrical parameters.

and Sorensen (*15*), however, have determined solutions as a function of $\lambda\dot{\gamma}$ using Galerkin's method. Unlike elongational flow, the solution varies with both θ and ϕ. The value of $\dot{\gamma}$ to use in the calculation will be estimated from the wall shear rate of an equivalent bundle of capillary tubes with radius R(*16*),

$$R = \frac{D_p \varepsilon}{3(1-\varepsilon)} = \frac{(25\ \mu\text{m})(0.4)}{3(0.6)} = 5.6\ \mu\text{m} \tag{9}$$

The shear rate for such a capillary is given by

$$\dot{\gamma} = \frac{4\bar{V}}{R} = \frac{4Q}{A\varepsilon R} = \frac{4\left(\frac{1}{60}\text{ cm}^3/\text{s}\right)}{\pi(0.23\text{ cm})^2(0.4)(5.6\ \mu\text{m})} = 1800\text{ s}^{-1} \tag{10}$$

where ε is the porosity
$\bar{V}$ is the average pore velocity
Q is the flow rate through the bed
A is the cross-sectional area of the bed

The product $\lambda\dot{\gamma}$ is therefore $\sim$10. Figure 9 is a plot of contours of constant ψ at $\lambda\dot{\gamma} = 10$, taken from Stewart and Sorensen's article. Since $\psi(\theta, \phi)$ is not symmetric with respect to the direction of flow, the definition of an effective radius is not as simple as in the case of elongational flow. A reasonable choice employs the position of the peak value of $\psi(\theta, \phi)$ to define D_{eff}. Figure

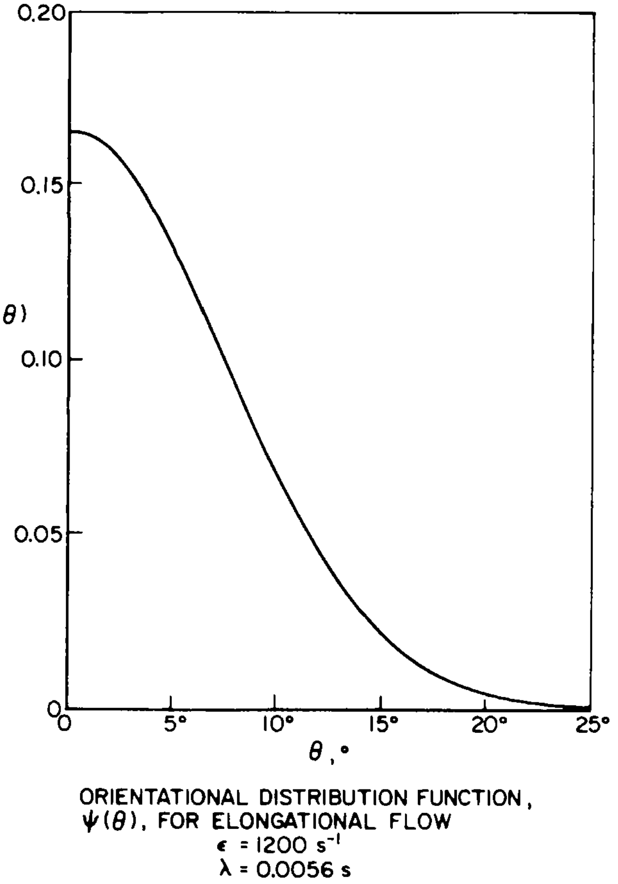

FIG. 7. Orientational distribution function, ψ, for elongational flow. The sharp peak of the orientational distribution function indicates strong alignment along streamlines. Note that the possibility of orientation further than 15° from streamline is very remote.

9 yields a maximum value of ψ at $\theta = 90^\circ$, $\phi = 13^\circ$. This corresponds to D_{eff} of about 0.22 μm, close to the value calculated for elongational flow.

CONCLUSIONS

Experimental results show that a xanthan molecule elutes from a hydrodynamic chromatography column with a retention time equal to that of a latex sphere of diameter 0.153 μm. This number agrees rather well with the

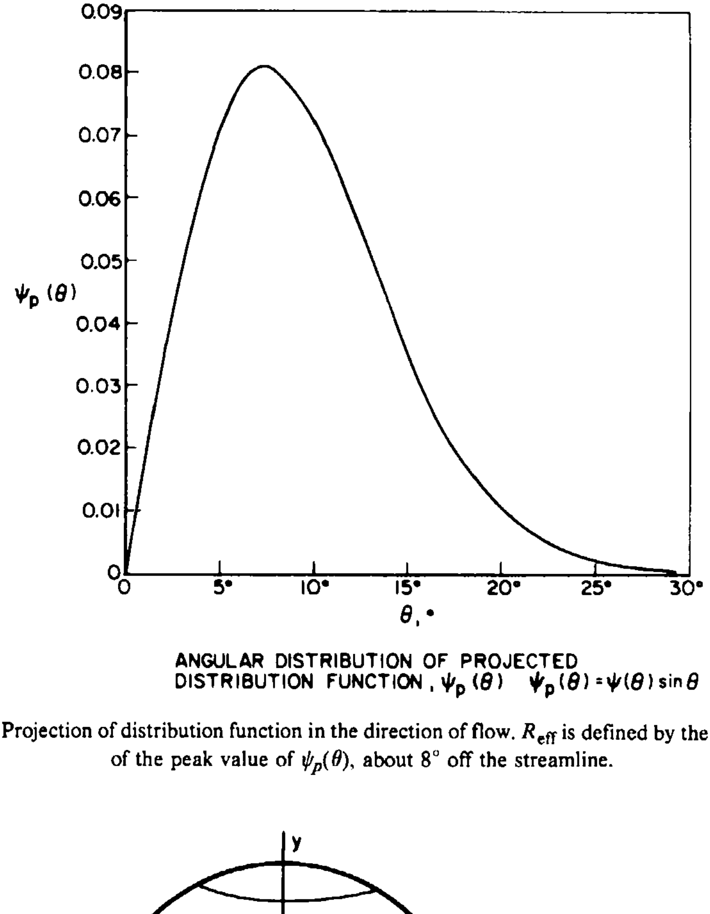

FIG. 8. Projection of distribution function in the direction of flow. R_{eff} is defined by the location of the peak value of $\psi_p(\theta)$, about 8° off the streamline.

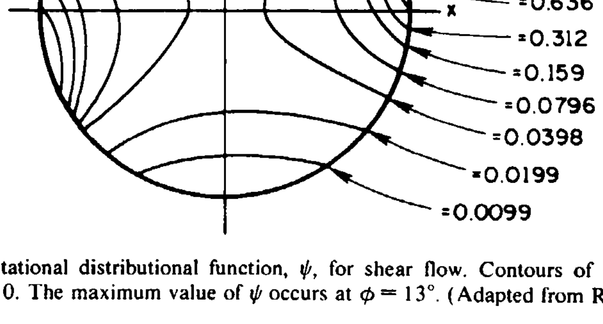

FIG. 9. Orientational distributional function, ψ, for shear flow. Contours of constant ψ at $\lambda\dot{\gamma} = 10$. The maximum value of ψ occurs at $\phi = 13°$. (Adapted from Ref. 15.)

approximate values of D_{eff} of xanthan for elongational and shear flows, 0.14 and 0.22 μm, respectively. Although the actual flow in a hydrodynamic chromatography column is neither pure shear nor pure elongation, the preceeding results are strong evidence that a rodlike molecule such as xanthan is closely oriented along streamlines during flow through the column. These results also indicate that D_{eff} is a significant parameter in characterizing the separation mechanism.

The orientation effect may have an important influence on the performance and design of hydrodynamic chromatography involving nonspherical particles. For example, in elongational flow,

$$D_{\text{eff}} \propto \sqrt{D_p/Q} \qquad (11)$$

From HDC studies on latex spheres it is known that optimum separations are obtained for certain ratios of packing size to latex sphere size. Equation (11) suggests that by varying the flow rate the apparent packing particle size can be changed for HDC separations of orientable particles. In effect, the column can be tuned to provide optimal separations by adjusting flow rate instead of having to change packings.

In addition, these calculations may provide a basis for interpreting the filtration of rodlike molecules through porous membranes and the permeability of rodlike macromolecules in porous media. For in both cases flow-induced orientation changes the dimensions of the molecule projected perpendicular to the axis of flow.

REFERENCES

1. R. K. Prud'homme, G. Froiman, and D. A. Hoagland, *Carbohydr. Res., 106*, 225 (1982).
2. G. Holzwarth, *Ibid., 66,* 173 (1978).
3. R. Moorhouse, M. Walkinshaw, and S. Arnot, in *Extracellular Microbial Polysaccharides* (T. Andrew, P. Sandford, and A. Laskin, eds.), *ACS Symp. Ser., 45,* 90 (1977).
4. F. R. Dintzis, G. E. Babcock, and R. Tobin, *Carbohydr. Res., 13,* 257 (1970).
5. J. Southwick, H. Lee, A. Jamieson, and J. Blackwell, *Ibid., 84,* 287 (1980).
6. H. Small, *J. Colloid Interface Sci., 48,* 147 (1974).
7. C. A. Silebi and A. J. McHugh, *AIChE J., 24,* 204 (1978).
8. D. J. Nagy, C. A. Silebi, and A. J. McHugh, *J. Appl. Polym. Sci., 26,* 1567 (1981).
9. S. Wellington, *Polym. Prepr.,* ACS Meeting, New York, 24–28, 1981.
10. G. Holzwarth and F. G. Prestridge, *Science, 197,* 757 (1977).
11. R. B. Bird, O. Hassager, R. C. Armstrong, and C. F. Curtiss, *Dynamics of Polymeric Liquids,* Vol. 2, *Kinetic Theory,* Wiley, New York, 1977, pp. 522–542.
12. H. Brenner, *Int. J. Multiphase Flow, 1,* 223 (1974).

13. A. C. Payatakes and M. A. Neira, *AIChE J.*, *23*, 922 (1977).
14. M. A. Neira and A. C. Payatakes, *Ibid.*, *24*, 43 (1978).
15. W. E. Stewart and J. P. Sorensen, *Trans. Soc. Rheol.*, *16*, 1 (1972).
16. R. B. Bird, W. E. Stewart, and E. N. Lightfoot, *Transport Phenomena*, Wiley, New York, 1960, p. 197.

Received by editor January 11, 1982
Revised July 27, 1982